

# measurements of Joule heating using SuperDARN and the SCANDI Fabry-Perot interferometer

D. D. Billett<sup>1</sup>, A. M. Ronksley<sup>2</sup>, A. Grocott<sup>1</sup>, A. Aruliah<sup>2</sup>, J. A. Wild<sup>1</sup>

d.billet@lancaster.ac.uk

<sup>1</sup> Lancaster University, <sup>2</sup> University College London

## 1. Introduction

- Joule heating is controlled by the frictional interactions of **charge carriers** (plasma) and **neutrals** in the high latitude thermosphere
- Ground based radar network, **SuperDARN**, can tell us about the plasma. The **SCANDI Fabry-Perot interferometer** tells us about the neutrals via auroral airglow emission.
- Examples of 2D, high spatio-temporal resolution Joule heating images have been created by finding events with high amounts of overlapping SuperDARN and SCANDI data
- SCANDI is located on **Svalbard** and most commonly operates in a 61 zone configuration, obtaining a maximum of up to **61 neutral wind vectors** using fitting techniques from Conde & Smith [1998].
- Two SuperDARN radars overlook Svalbard, **Hankasalmi** in Finland and **Pykkvibaer** in Iceland. These provide the fitted plasma velocities.

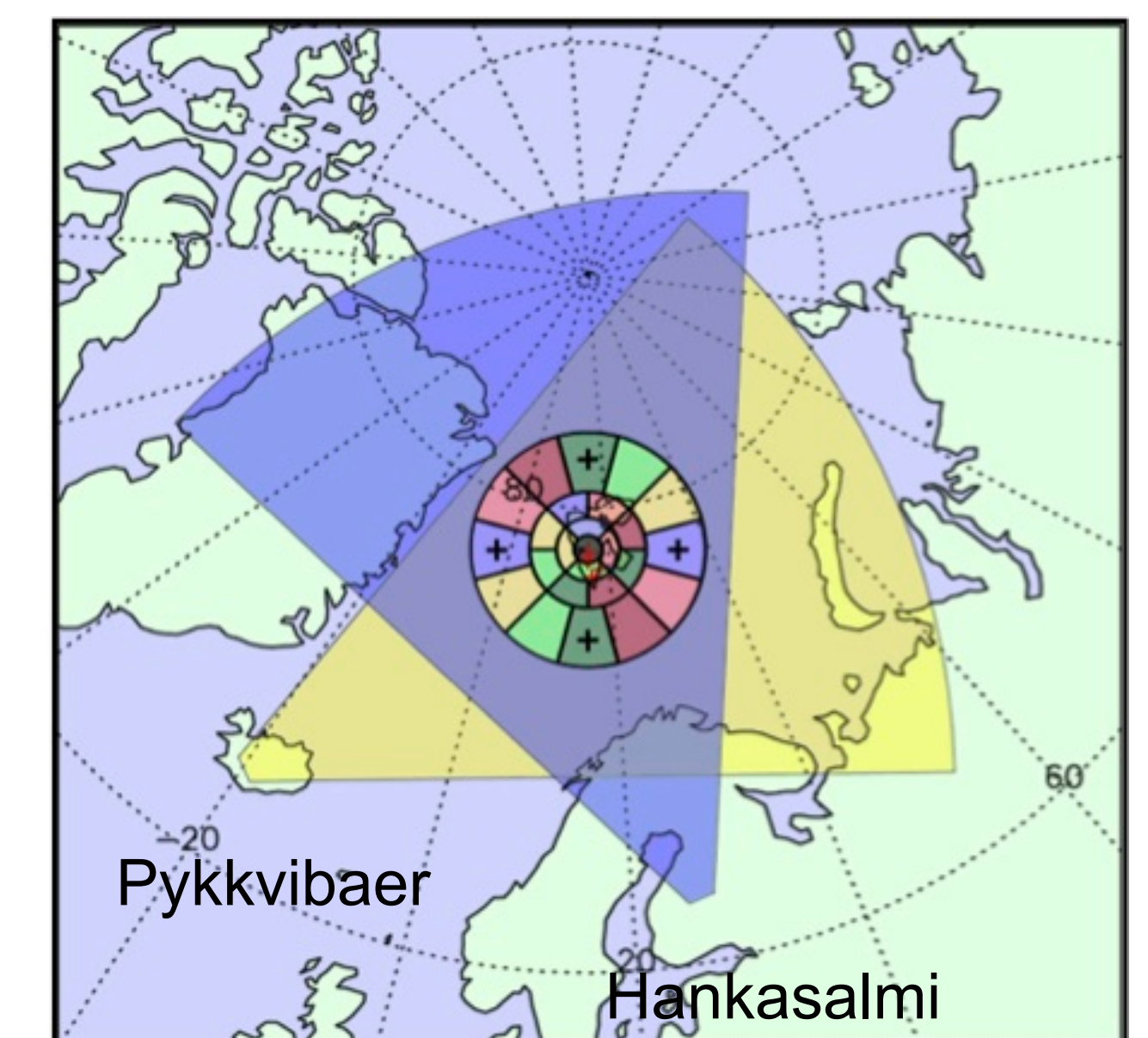


Figure 1. SCANDI and SuperDARN locations adapted from Aruliah et al. [2009]

## 2. Coverage

- SCANDI has been in operation since 2007, allowing 10 years of **winter-time data**
- There are not always direct SuperDARN velocity measurements in the SCANDI FOV, but we use the SuperDARN “map potential” technique to intelligently interpolate over areas without data [Ruohoniemi & Baker, 1998].
- After filtering SCANDI data for clear skies and goodness of fit ( $0.5 < \chi^2 < 1.5$ ), the number of SuperDARN plasma vectors in the SCANDI FOV is shown in figure 2.

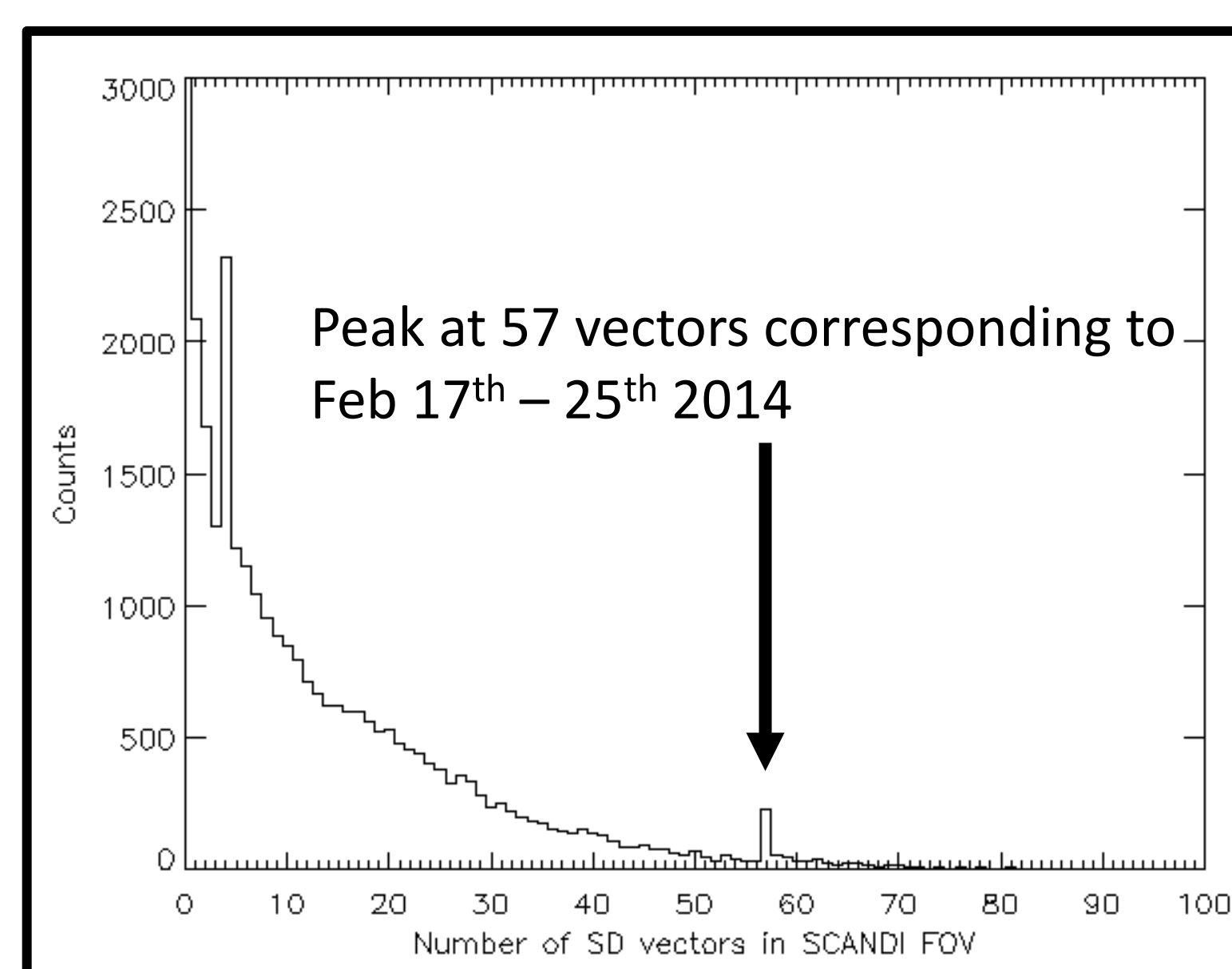


Figure 2. The number of measured SuperDARN plasma vectors within the SCANDI FOV for a filtered dataset. There is a peak labelled which corresponds to 8 consecutive days of excellent data coverage for both SuperDARN and SCANDI.

## 3. Calculation

$$\Sigma Q_J = \Sigma_P E^2 + 2\Sigma_p \mathbf{E} \cdot (\mathbf{V}_n \times \mathbf{B}) + \Sigma_p (\mathbf{V}_n \times \mathbf{B})^2$$

- $\Sigma Q_j$  - Height Integrated Joule heating
- $\mathbf{E}$  - Electric field from SuperDARN:  $\mathbf{E} = -\mathbf{V} \times \mathbf{B}$
- $\mathbf{V}_n$  - Neutral winds from SCANDI
- $\mathbf{B}$  - Magnetic field from IGRF model [Thébault et al., 2015]
- $\Sigma_p$  - Pedersen conductivity from Solar zenith model [Rich et al., 1987] and auroral model [Hardy et al., 1987].
- Joule heating is increased the stronger the difference between the neutral and plasma velocities are.

## 4. February 21<sup>st</sup>, 2014 Event – Neutral flow switch

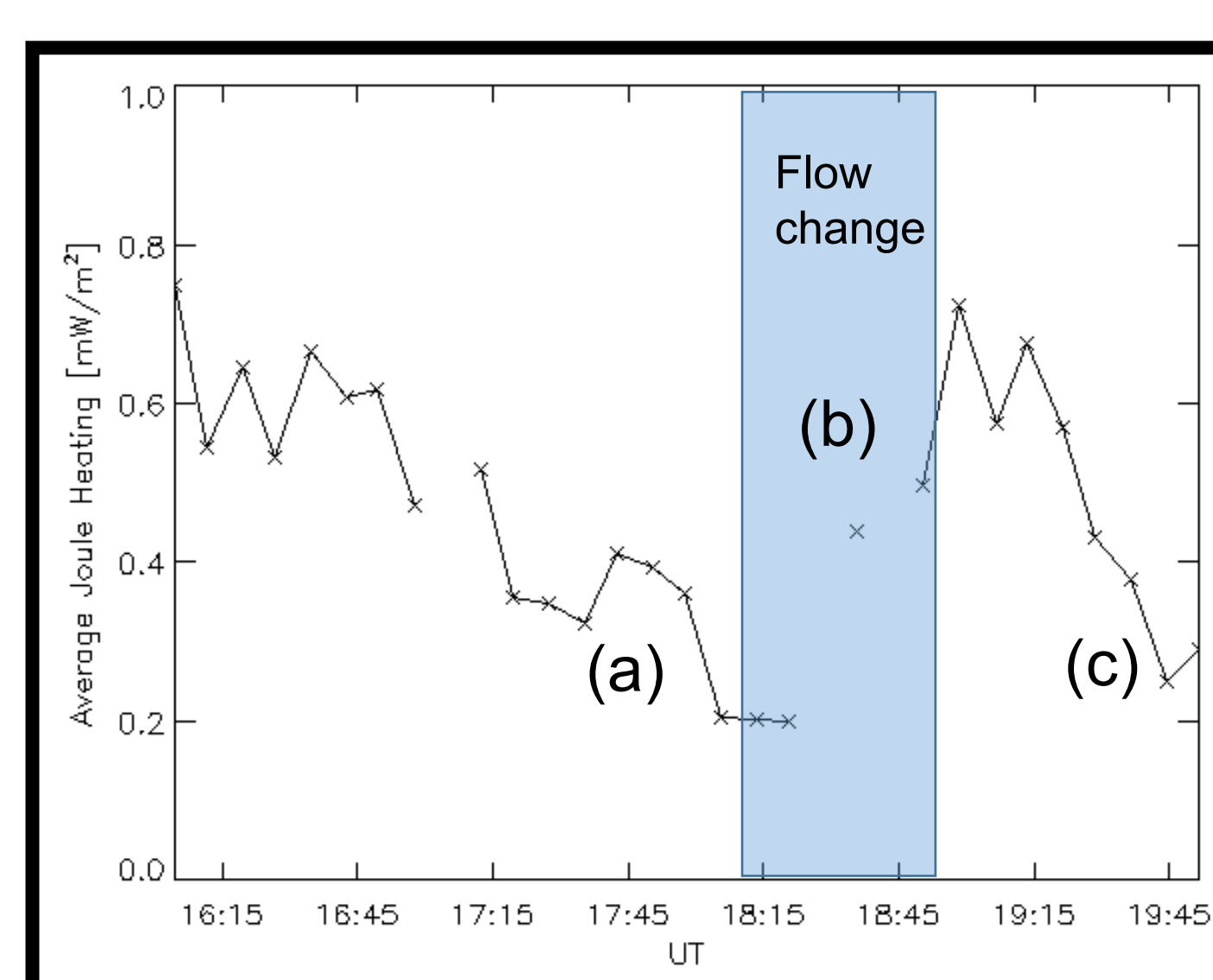
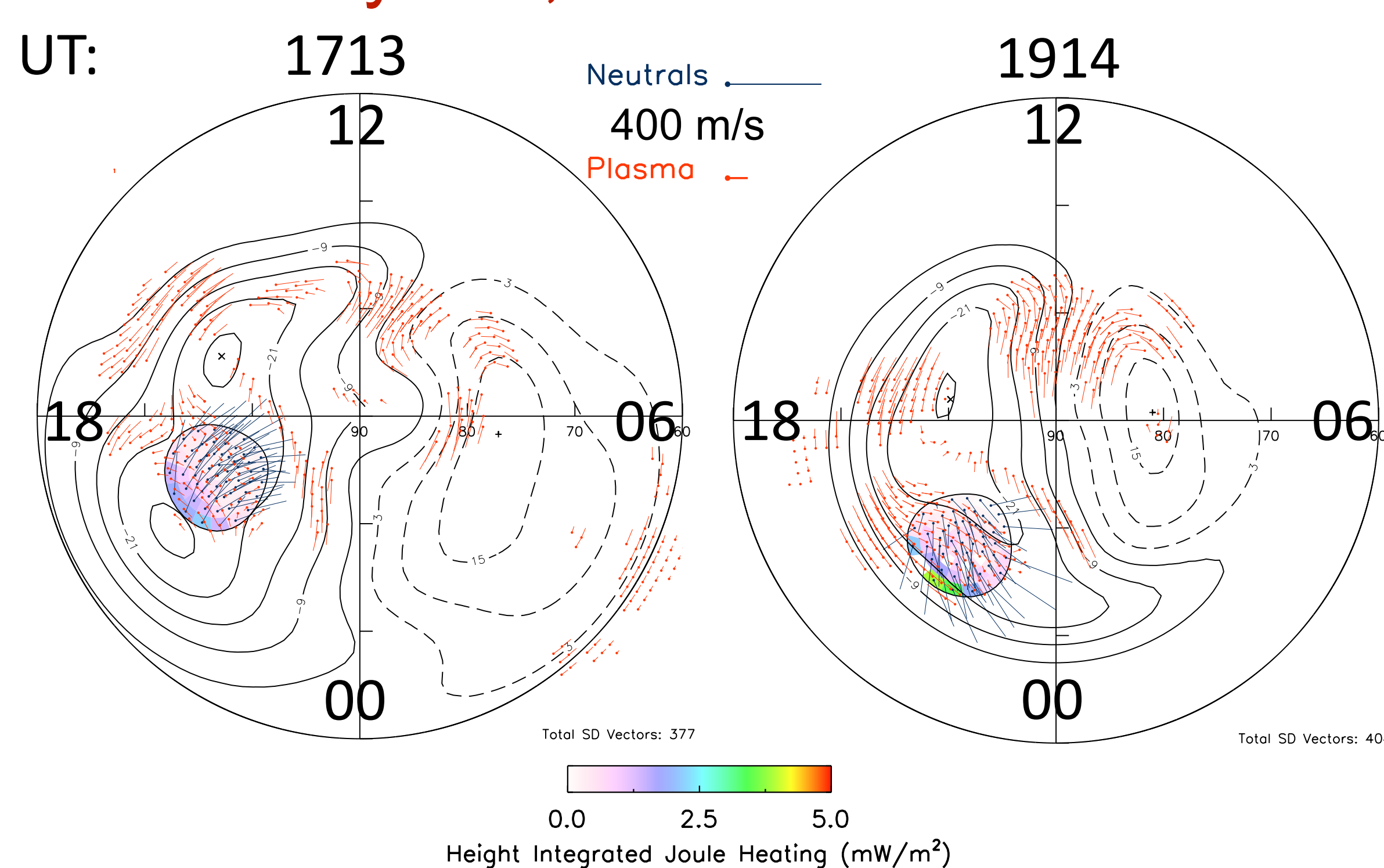
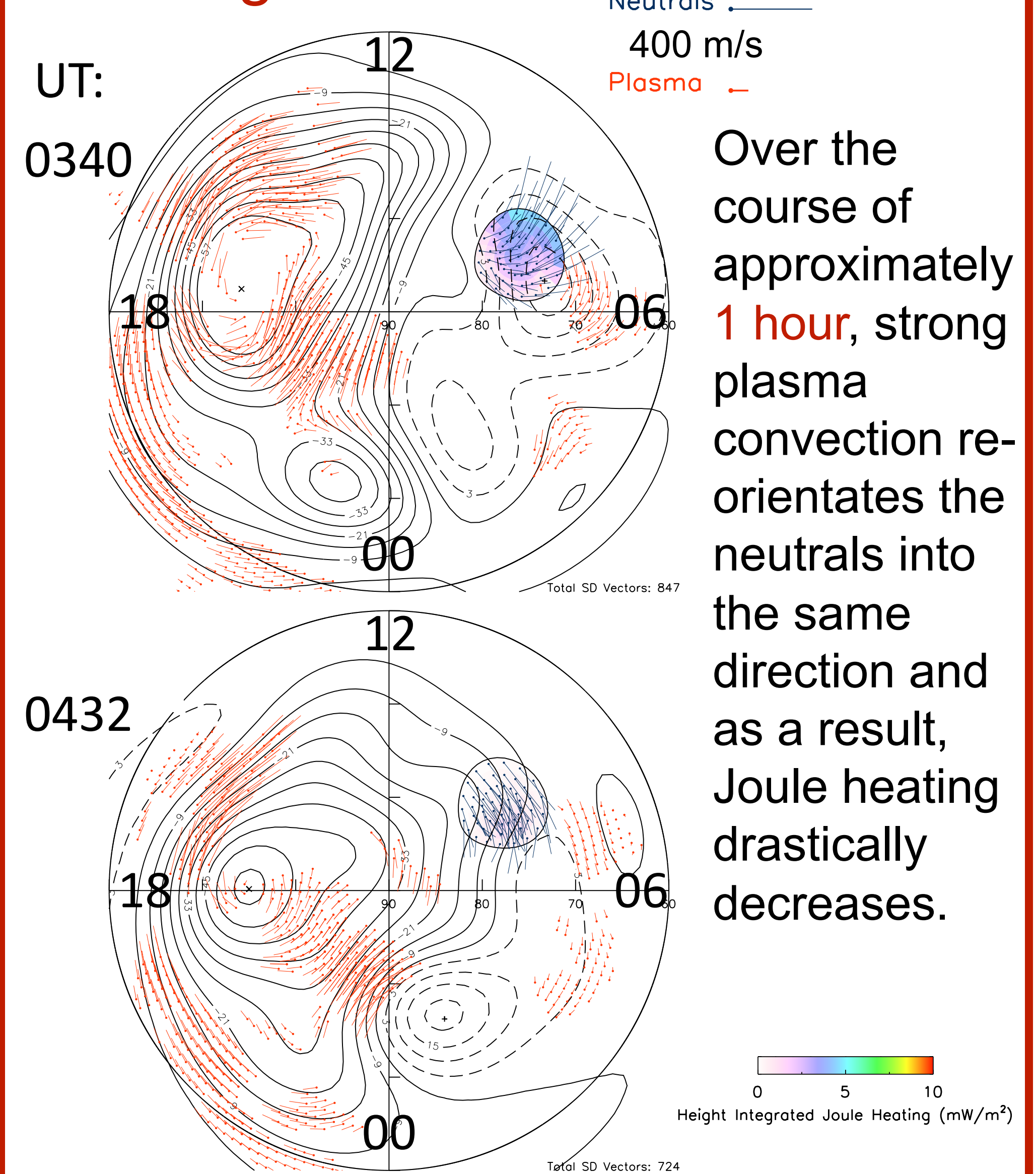


Figure 3. A time series of how the average Joule heating changes within the SCANDI FOV.

- The decrease in Joule heating indicates neutrals pulled into direction of plasma via ion-drag – (a), (c) in Figure 3.
- The sudden change of neutral direction increases Joule heating, especially at lower latitudes – (b) in Figure 3.
- This indicates some stronger control over neutrals than ion-neutral drag, such as **Coriolis** forces or **solar pressure gradients** driving the neutrals from the plasma configuration and increasing Joule heating. This is significant because ion-neutral drag is often seen as the dominant force affecting neutrals.

## 5. December 7<sup>th</sup>, 2013 Event – Ion drag in action



Over the course of approximately **1 hour**, strong plasma convection re-orientates the neutrals into the same direction and as a result, Joule heating drastically decreases.

## References

Conde, M., & Smith, R. W. (1998). Spatial structure in the thermospheric horizontal wind above Poker Flat, Alaska, during solar minimum. *Journal of Geophysical Research: Space Physics*, 103(A5), 9449-9471.  
 Hardy, D. A., M. Gussenhoven, R. Raistrick, and W. McNeil (1987). Statistical and functional representations of the pattern of auroral energy flux, number flux, and conductivity. *Journal of Geophysical Research: Space Physics*, 92(A11), 12,275-12,294.  
 Rich, F. J., M. Gussenhoven, and M. E. Greenspan (1987). Using simultaneous particle and field observations on a low-altitude satellite to estimate joule heat energy flow into the high-latitude ionosphere. *Tech. rep.*, Air Force Geophysics Lab., Hanscom AFB, MA (USA).  
 Ruohoniemi, J. M., & Baker, K. B. (1998). Large-scale imaging of high-latitude convection with Super Dual Auroral Radar Network HF radar observations. *Journal of Geophysical Research: Space Physics*, 103(A9), 20797-20811.  
 Thébault, E., Finlay, C. C., Beggan, C. D., Alken, P., Aubert, J., Barrois, O., ... & Canet, E. (2015). International geomagnetic reference field: the 12th generation. *Earth, Planets and Space*, 67(1), 79.

## 6. Future work

- Using the full overlapping SuperDARN and SCANDI data sets, a statistical analysis of Joule heating in the 70-80° magnetic latitude range will be performed and compared to previous modelling efforts.
- All-sky auroral emission data can be used to derive high resolution 2D conductivities as a replacement for statistical models.